A global view of one-dimensional solar radiative transfer through oceanic water clouds

Larry Di Girolamo,[1] Lusheng Liang,[1] and Steven Platnick[2]

Received 27 May 2010; revised 9 July 2010; accepted 13 July 2010; published 24 September 2010.

[1] Solar radiative transfer through a cloudy atmosphere is commonly computed assuming clouds to be one-dimensional, i.e., plane-parallel. Here we provide a global perspective on how often and with what degree oceanic water clouds may be considered plane-parallel by fusing multi-view-angle and multi-spectral satellite data. We show that the view-angular distribution of the retrieved reflectance, spherical albedo and cloud optical thickness measured at 1 km resolution are indistinguishable from plane-parallel clouds 24%, 25% and 79% of the time, respectively, at the 95% confidence level of our measurement method. These plane-parallel clouds occur most frequently within regions dominated by stratiform clouds under solar zenith angles <60°. For all other regions or sun-angles, the frequency in which clouds are indistinguishable from plane-parallel drops sharply to as low as a few percent. Our results provide a basis for interpreting space-time variability within many satellite-retrieved variables and reveal a need for continued efforts to handle three-dimensional radiative transfer in environmental modeling and monitoring systems. **Citation:** Di Girolamo, L., L. Liang, and S. Platnick (2010), A global view of one-dimensional solar radiative transfer through oceanic water clouds, *Geophys. Res. Lett.*, *37*, L18809, doi:10.1029/2010GL044094.

1. Introduction

[2] Clouds, which cover about 68% of the globe, regulate the incident solar radiation field in space and time more than any other atmospheric variable, and they act as a primary greenhouse constituent in our atmosphere. Our ability to accurately compute the interaction of the radiation field with clouds is critically important in the geosciences, including, for example, our ability to predict climate change, to quantify the climate forcing by anthropogenic aerosols through its influence on cloud microphysics, to produce accurate predictions of biogeochemical cycles and the oxidative capacity of our atmosphere, and to monitor environmental change from space [e.g., *Intergovernmental Panel on Climate Change*, 2007]. By assuming clouds and their radiative boundary conditions to be plane-parallel, the transfer of solar radiation is greatly simplified to one-dimension (the vertical). This makes radiative transfer calculations computationally fast and solutions to the inverse problem faced in satellite remote sensing tangible. However, a simple look at clouds, either from the ground, aircraft or spacecraft reveals that they are often not horizontally homogenous over a wide range of scales, thereby raising questions as to the degree to which the plane-parallel assumption produces the required accuracy for various applications.

[3] Many studies have given important insight into the applicability of the plane-parallel assumption, showing significant errors in calculating radiative-heating and photochemical-reactions, or on satellite remote sensing when applied to heterogeneous cloud fields [e.g., *Loeb and Davies*, 1996; *Chambers et al.*, 1997; *Zuidema and Evans*, 1998; *O'Hirok and Gautier*, 2005; *Bouet et al.*, 2006; *Marshak et al.*, 2006; *Kato and Marshak*, 2009]. Most of these have been either derived over a limited regional domain from observations or from computationally expensive 2- or 3-D radiative transfer calculations applied to only a few simulated heterogeneous cloud fields. The extent to which the results from these studies are globally applicable requires measureable deviations from 1-D solar radiative transfer for real clouds from global observations.

[4] This letter provides such measureable deviations from global satellite observations of marine water clouds using a novel approach that we recently developed and tested on a limited regional dataset derived from the Multiangle Imaging SpectroRadiometer (MISR) and the Moderate Resolution Imaging Spectroradiometer (MODIS) instruments [*Liang et al.*, 2009]. Our data and method are presented in Section 2. Sections 3 and 4 present our results and error analysis, respectively. The broader implications of our results and recommendations for future research are provided in Section 5.

2. Data and Method

[5] The MISR and MODIS instruments are onboard NASA's *Terra* satellite, which is in a sun-synchronous, ~10:30 AM equator-crossing-time orbit. Our analysis is confined to liquid water clouds, as determined from the MODIS cloud phase product, over ice-free ocean using data collected between 2001 and 2008 for the months of January and July. We used Collection 5 of the MODIS data and Version 24 of the MISR radiances that are available as bidirectional reflectance factors (BRF). Only the MODIS data that falls within the MISR swath are used in our analysis.

[6] Our method is fully detailed by *Liang et al.* [2009]. In brief, fusion of the data from MODIS and the multiple camera views from MISR are done at cloud-top and at pixel resolution (~1 km), and the analysis is confined to the seven MISR cameras that view the clouds within 60° of nadir. Only those domains that are fully cloudy and that have passed the registration quality controls detailed by *Liang et al.* [2009] are used in this analysis. Cloud optical thickness is retrieved using the near-infrared BRF from the MISR nadir camera and

[1]Department of Atmospheric Sciences, University of Illinois at Urbana-Champaign, Urbana, Illinois, USA.
[2]Laboratory for Atmospheres, NASA Goddard Space Flight Center, Greenbelt, Maryland, USA.

Copyright 2010 by the American Geophysical Union.
0094-8276/10/2010GL044094

effective radius from MODIS, based on the same plane-parallel radiative transfer model used to construct the look-up tables in the MODIS cloud optical thickness and effective radius retrievals [*Platnick et al.*, 2003]. If the clouds are truly plane-parallel and all other assumptions used by MODIS in retrieving the cloud microphysical properties are valid, then substituting the retrieved optical thickness and effective radius back into the radiative transfer code to produce simulated MISR BRFs for the off-nadir cameras should match with the observed MISR BRFs [*Liang et al.*, 2009]. Let R_i^{sim} and R_i^{obs} represent the 3 × 3 domain mean 866 nm channel radiance simulated for and observed by MISR, respectively, where i is the MISR camera index ($i = \{1, 2, \ldots, 7\}$). If clouds are plane-parallel, then we expect the relative difference between R_i^{sim} and R_i^{obs}, $\delta R_i = \frac{R_i^{sim} - R_i^{obs}}{R_i^{obs}}$, to be close to zero for all i. Overall angular consistency is quantified by, m_{BRF}, defined as

$$m_{BRF} = \sqrt{\frac{1}{7}\sum_{i=1}^{7}\left(\frac{R_i^{sim} - R_i^{obs}}{R_i^{obs}}\right)^2} \times 100\%.$$

[7] Alternatively, if clouds are plane-parallel, then satellite-derived cloud properties, such as optical thickness, effective radius and albedo should be independent of the viewing geometry of the satellite instrument. Using the effective radii retrieved from MODIS and the MISR observed BRF, the cloud optical thickness and spherical albedo are retrieved for each MISR camera following the procedures of *Liang et al.* [2009]. The coefficient of variation of the retrieved optical thickness, m_τ, and spherical albedo, m_β, are defined as:

$$m_x = \frac{1}{\langle x_i \rangle}\sqrt{\frac{1}{7-1}\sum_{i=1}^{n}(x_i - \langle x_i \rangle)^2} \times 100\%,$$

where, x_i is either the mean cloud optical thickness or spherical albedo over a domain in the ith MISR camera and $\langle\ \rangle$ denotes averaging over the seven MISR cameras.

[8] Ideally, these measures of angular consistency are zero for plane-parallel clouds. In practice, they are greater than zero due to factors other than the plane-parallel assumption, including the MISR camera-to-camera relative calibration and the assumptions used by the MODIS algorithm to retrieve cloud optical thickness and effective radii (e.g., an assumed vertically homogeneous distribution of cloud microphysical properties and an assumed Lambertian surface). In Section 4, we estimate the upper limit of the 95% confidence interval for plane-parallel values of m_{BRF}, m_τ, and m_β to be $m_{BRF}(95\%) = 2.32\%$, $m_\tau(95\%) = 14.41\%$, and $m_\beta(95\%) = 2.24\%$. Thus, measured values of m_{BRF}, m_τ, and m_β that are less than $m_{BRF}(95\%)$, $m_\tau(95\%)$, and $m_\beta(95\%)$ are indistinguishable from plane-parallel values at the 95% confidence level. The larger uncertainty in m_τ relative to m_{BRF} and m_β is attributed to the non-linear relationship between cloud optical thickness and measured BRF.

3. Results

[9] Figure 1 shows the probability distribution functions (PDF) and cumulative PDFs in the occurrence of measured m_{BRF}, m_τ, and m_β accumulated for the months of January and July from 2001 to 2008. Figure 1 reveals, for example, that clouds are angularly consistent (cumulative frequency) in BRF, optical thickness and spherical albedo at the 95% confidence level with their plane-parallel value (e.g., $m_{BRF} \leq 2.32\%$) 26.7%, 83.6%, and 22.5% of the time, respectively, for January and 22.1%, 75.1%, and 26.7% of the time, respectively, for July. These numbers are tied directly to our method's ability to detect plane-parallel angular inconsistency in BRF, optical thickness and spherical albedo; whether these detection values are too strict or not strict enough depends on the requirements of the intended application. For example, it has been suggested that a better than 5% accuracy in measured radiative cloud properties from satellites is required for climate research [*Ohring et al.*, 2005]. Figure 1 shows clouds to be angularly consistent 67.4%, 22.5%, and 71.4% of the time, respectively, for January and 61.6%, 23.1%, and 61.2% of the time, respectively, for July for m_{BRF}, m_τ, and $m_\beta < 5\%$, respectively. Connecting angular consistency with uncertainty is discussed in Section 4.

[10] While the PDFs in Figure 1 are similar for January and July, differences in their regional distributions can be very large. Figure 1 shows the regional distributions in the frequency (passing rate) in which $m_{BRF} < m_{BRF}(95\%)$ and $m_{BRF} < 5\%$. The solar zenith angles at the time of observations, which are tied to *Terra*'s sun-synchronous orbit, are also shown in Figure 1. We see that the spatial distribution of passing rates appears to be tied to two key factors: the spatial distribution of stratiform clouds and the solar zenith angle. It has been well documented that marine stratiform clouds appear frequently off the subtropical western coasts of continents, most prevalently off the coasts of California, Peru, and Angola, as well as regions of mid- to high-latitude lows. While high passing rates appear off these coasts in both January and July, the mid- to high-latitude lows have high passing rates only in the summer hemisphere, when solar zenith angles are smaller compared to the winter hemisphere. A transition in passing rates is evident as we move from the subtropical stratus to mid-latitudes at a solar zenith angle ~60° in the winter hemisphere. For solar zenith angles >60°, the passing rates drop to very low values, despite the stratiform nature of clouds found at these latitudes. These two effects are also evident in passing rates associated with m_τ and m_β in Figures S1 and S2 of the auxiliary material.[1]

[11] To better understand the regional distributions of m_{BRF}, m_τ, and m_β and quantify their relationship with the cloud heterogeneity, we examined the spatial heterogeneity metric, H_σ, proposed by *Liang et al.* [2009]. H_σ is equal to σ/R, where R and σ are the mean and standard deviation, respectively, of the 866-nm BRF calculated from the local group of 275-m 12 × 12 pixels from the MISR nadir camera centered on the 1km region under analysis. The regional distributions of mean H_σ are also shown in Figure 1. As expected, some of the most locally homogeneous regions (small values of H_σ) appear off the subtropical western coasts of continents, where marine stratocumulus clouds dominate. Unexpected, however, is the dichotomy in cloud homogeneity at mid- to high-latitudes between the winter and summer hemisphere, with the summer hemisphere appearing much more locally homogeneous compared to the winter hemisphere. It may be that the summer hemisphere clouds are physically smoother (e.g., less bumpy cloud-tops) compared

[1]Auxiliary materials are available in the HTML. doi:10.1029/2010GL044094.

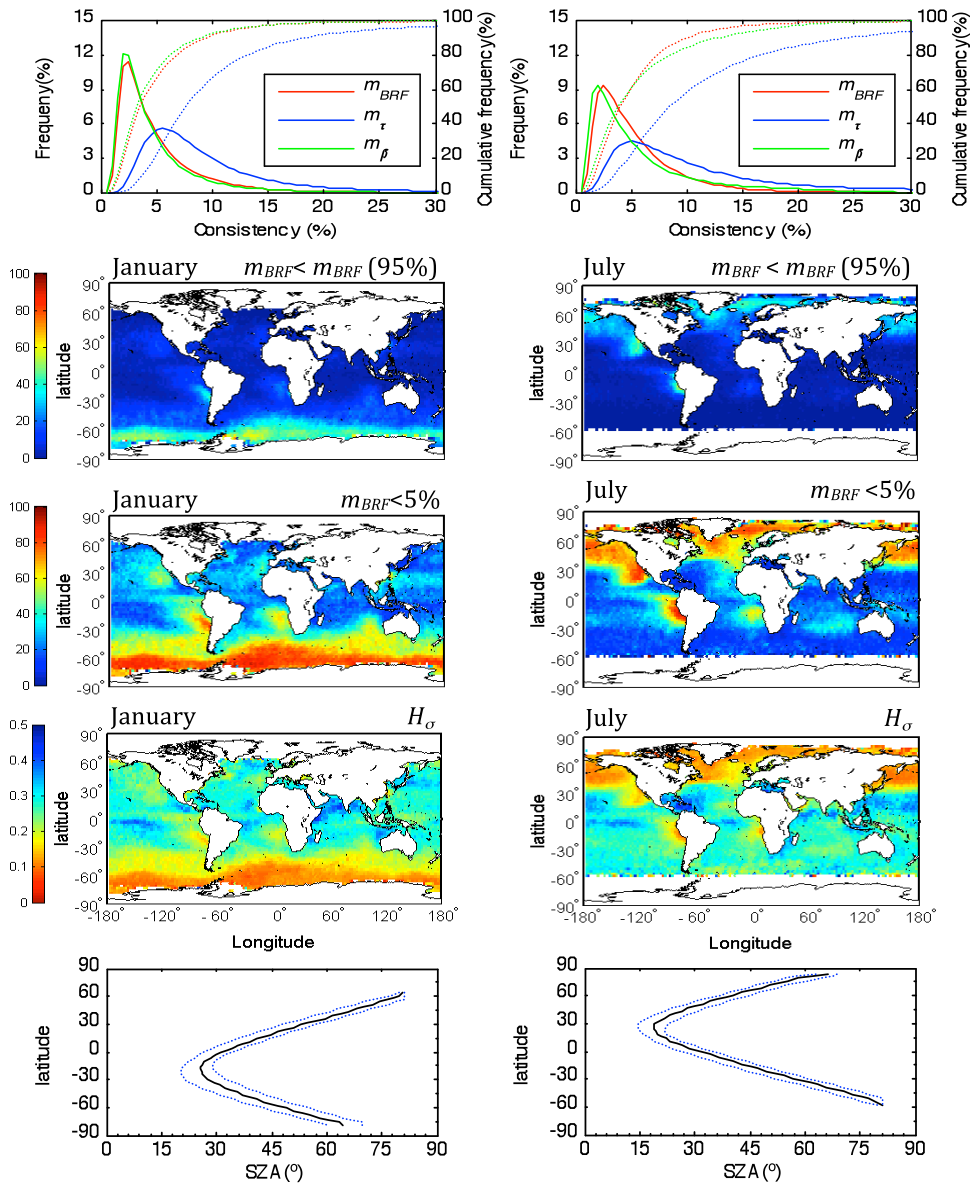

Figure 1. From top to bottom, PDFs and cumulative PDFs for m_{BRF}, m_τ and m_β; the frequency in which m_{BRF} are within the 95% confidence level of their plane-parallel value (m_{BRF}(95%)=2.32%); the frequency in which m_{BRF} < 5%; the spatial heterogeneity parameter, H_σ; and the mean solar zenith angle (SZA) as a function of latitude (enveloped by the maximum and minimum SZA). (left) For January and (right) for July.

to the winter hemisphere clouds. It may also be a solar zenith angle effect on H_σ: clouds can appear smoother under high Sun due to a net horizontal transport of sunlight from thicker regions to thinner regions of the clouds [e.g., *Zuidema and Evans*, 1998], whereas they can appear rougher for low Sun due to the illumination and shadowing of cloud sides [e.g., *Várnai and Marshak*, 2003]. However, when comparing regions under the same solar zenith angles, smaller H_σ represents physically smoother clouds.

[12] Comparing m_{BRF} (and m_τ and m_β in Figures S1 and S2) with H_σ reveals that larger deviations from plane-parallel occur for larger apparent cloud heterogeneity. This is quantified in Figure 2a, which shows the 2-D distribution between m_{BRF} and H_σ for July (Figure S3 for January and for m_τ and m_β). This figure looks remarkably similar when stratified by solar zenith angle (not shown). As the cloud becomes more spatially heterogeneous (i.e., as H_σ increases), the median and spread of m_{BRF}, m_τ, and m_β become larger. Analysis of Figure 2a and Figure S3 reveals that the 10% most spatially homogeneous clouds (H_σ < 0.05) have m_{BRF} < 7.0%, m_τ < 27.4%, and m_β < 9.5% almost all of the time. For the 10% most spatially heterogeneous domains (H_σ > 0.326), m_{BRF}, m_τ, and m_β are less than m_{BRF}(95%), m_τ(95%), and m_β(95%) for 0.5%, 49.2%, and 1.2% of the time, respectively. Note, Figure 2a shows some very homogeneous clouds (H_σ < 0.02) with large values of m_{BRF}. We traced these rare occurrences to smoke overlying cloud — a scenario that invalidates the assumption used in the MODIS cloud property retrieval algorithm.

[13] The relationship between m_{BRF}, m_τ, m_β and H_σ allows us to use H_σ alone to identify pixels that meet a specified requirement for the cloud to be considered plane-parallel.

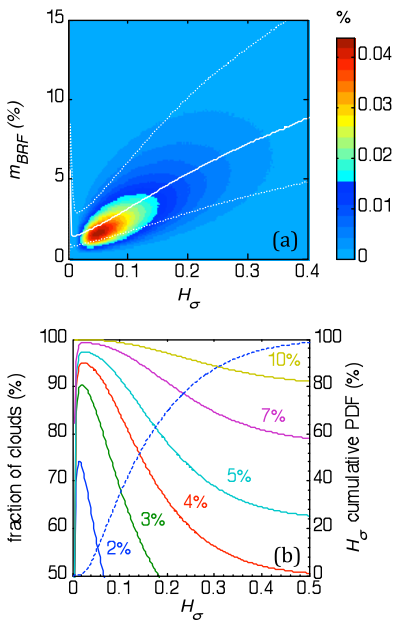

Figure 2. (a) Two-dimensional frequency distribution of m_{BRF} and H_σ for July. Also plotted are the median (solid thick line), 10th and 90th percentile (dotted lines) of m_{BRF} computed over H_σ bin intervals of 0.004. (b) The fraction of cloud observations that are less than m_{BRF} (for m_{BRF}–values ranging from 2% to 10%) and H_σ for July. The dash line is the cumulative PDF of H_σ.

Figure 2b shows the threshold in H_σ required to have a certain percentage of data meet a certain value of m_{BRF} for July. Similar plots are given in Figures S3 and S4 for m_τ and m_β for July and for all three angular metrics for January. For example, (i) requiring 90% of the retrievals to be angularly consistent in BRF to within 5% of their plane-parallel value (i.e., $m_{BRF} < 5\%$) suggests performing retrievals only where $H_\sigma < 0.112$ — 40% of domains met this criterion; (ii) requiring $m_\tau < 15\%$ for 90% of the retrievals suggests performing retrievals only where $H_\sigma < 0.088$ — 29% of the domains met this criteria; and (iii) requiring $m_\beta < 5\%$ for 90% of the retrievals suggests performing retrievals only where $H_\sigma < 0.076$ — 23% of the domains met this criteria. Placing a strict criterion for plane-parallel clouds allows greater confidence in the microphysical retrievals and their estimate of uncertainty as reported in the MODIS product [*Platnick et al.*, 2004]. Since the relationships between H_σ and the angular consistency metrics are largely insensitive to solar zenith angle, the H_σ thresholds based on Figure 2b may be applicable to the historic record of MODIS and other MODIS-like instruments on other platforms.

4. Error Assessment

[14] As mentioned in Section 2, uncertainties in our data and method leads to non-zero values of m_{BRF}, m_τ, and m_β even for truly plane-parallel clouds. Under the assumption that spatially homogeneous clouds are plane-parallel, we can estimate the total error in m_{BRF}, m_τ, and m_β by examining the distribution of m_{BRF}, m_τ, and m_β in the limit that H_σ goes to zero. By using the data shown in Figures 2a, S3, and S4, and choosing the smallest H_σ bin that has more than 100,000 samples (H_σ = 0.012–0.014), the distributions of m_{BRF}, m_τ, and m_β, summed from the January and July data, are taken to represent their error distributions. The 68% confidence level of these distributions occur at $m_{BRF}(68\%) = 1.69\%$, $m_\tau(68\%) = 7.89\%$, and $m_\beta(68\%) = 1.65\%$, and their 95% confidence level occur at $m_{BRF}(95\%) = 2.32\%$, $m_\tau(95\%) = 14.41\%$, and $m_\beta(95\%) = 2.24\%$. These estimates are likely biased high given that we assumed that small H_σ behave perfectly as plane-parallel clouds.

[15] It is tempting to interpret m_{BRF}, m_τ, and m_β as a direct measure of accuracy in our ability to simulate the BRF or to retrieve τ and β. However, they should not be; they simply quantify the view-angular consistency in BRF, τ, and β relative to their plane-parallel expectation [*Liang et al.*, 2009]. Only if, for example, the retrieved cloud optical thickness at each MISR view-angle were independent, with no errors that depend systematically on view-angle, could we interpret m_τ as an estimate of the random error in our ability to measure the cloud optical thickness. That the spatial heterogeneity of clouds is known to lead to large systematic errors in τ-retrievals with view angle [e.g., *Várnai and Marshak*, 2007] precludes us from interpreting m_τ as an estimate of the random error, except perhaps in the limit that spatial heterogeneity (H_σ) goes to zero. In this limit, $m_\tau(68\%) = 7.89\%$, which is very close, but biased high as noted above, to the plane-parallel theoretical limit of 7.5% for our dataset as reported within the MODIS product [*Platnick et al.*, 2004]. This result essentially validates the plane-parallel cloud optical depth uncertainty reported in the MODIS product.

[16] The frequency in which clouds may be qualified as plane-parallel reported in this study may be biased because some water clouds in the months of January and July were excluded from our analysis. There were two reasons for this exclusion. The first reason is that the quality control criteria for registering clouds across multiple views can reject clouds for further analysis; this will bias the reported passing rates low by less than 1% using m_{BRF}, m_τ, or m_β [*Liang et al.*, 2009]. The second reason is that the MODIS 1km cloud optical property retrievals for Collection 5 omit cloudy pixels lying at the edge of detectable cloud fields and, to a lesser extent, those ocean pixels appearing to be partly cloudy according to the two higher resolution (250m) MODIS visible/near-infrared channels; hence such pixels are not included in our analysis. These pixels, which respectively represent 11% and 15% of all oceanic water clouds detected by MODIS in January and July, are excluded from MODIS processing because they are expected to have large deviations from plane-parallel radiative transfer due to cloud-side illumination and photon leakage [e.g., *Várnai and Marshak*, 2003]. The exclusion of these pixels in our analysis leads to optimistic estimates for the fraction of all cloud-filled pixels that may be qualified as plane-parallel, but is perfectly consistent with the subset of pixels used for MODIS cloud retrievals.

5. Recommendations

[17] Our results provide a basis for interpreting the space-time variability within many geophysical variables derived from satellite measurements of scattered sunlight. Applying the plane-parallel assumption to heterogeneous cloud fields are known to produce systematic errors (biases) in these geophysical variables [e.g., *Loeb and Davies*, 1996; *Chambers et al.*, 1997; *Marshak et al.*, 2006; *Kato and Marshak*, 2009],

which remain even after aggregating into monthly-averaged datasets. From these datasets, one cannot disentangle true space-time variability of the geophysical variable from variability in the biases caused by the plane-parallel assumption. The global maps shown in Figure 1 provide a starting point for disentangling these two sources of variability, since m_{BRF} and H_σ parallel the space-time variability of the biases. We recommend that 3-D radiative transfer simulations be undertaken over a range of cloud heterogeneity and solar zenith angles to quantify biases in terms of H_σ, so as to account for the magnitude of the biases in the satellite data. Correcting the biases will also be required for improving climate and environmental predictions models, where these models are often verified and tuned against satellite measurements derived from scattered sunlight.

[18] In carrying out pixel-scale analyses using the MODIS cloud microphysical products, we recommend using H_σ as a guide in selecting which cloud microphysical retrievals to place greater confidence in, as discussed in Section 3. These selected pixels are prime candidates for scientific analyses, since we have validated their associated plane-parallel uncertainty estimates as reported in the MODIS product. Note, however, that pixels with low H_σ are unlikely to be a random sample of all clouds.

[19] Finally, based on the results presented herein, we recommend that a much more concentrated effort be undertaken to develop the next generation of operationally viable remote sensing techniques to fully realize the 3-D radiative transfer found in nature, and for environmental models to push towards 3-D radiative transfer in calculating solar heating and photolysis rates. The later is limited by computational resource, whereas the former is limited by a missing theoretical foundation for the type of inverse problem at hand and by adequate satellite technology.

[20] **Acknowledgments.** We are grateful to the NASA Langley Research Center Atmospheric Sciences Data Center and the NASA Goddard Space Flight Center Atmosphere Archive Distribution System for archiving and distributing the MISR and MODIS datasets. Funding was provided by NASA through the New Investigator Program and the Earth and Space Science Fellowship Program, as well as through the MISR project managed by the Jet Propulsion Laboratory of the California Institute of Technology.

References

Bouet, C., F. Szczap, M. Leriche, and A. Benassi (2006), What is the effect of cloud inhomogeneities on actinic fluxes and chemical species concentrations, *Geophys. Res. Lett.*, *33*, L01818, doi:10.1029/2005GL024727.

Chambers, L. H., B. A. Wielicki, and K. F. Evans (1997), Accuracy of the independent pixel approximation for satellite estimates of oceanic boundary layer cloud optical depth, *J. Geophys. Res.*, *102*, 1779–1794, doi:10.1029/96JD02995.

Intergovernmental Panel on Climate Change (2007), *Climate Change 2007: The Physical Science Basis. Contributions of Working Group I to the Fourth Assessment Report of the Intergovernmental Panel on Climate Change*, edited by S. Solomon et al., Cambridge Univ. Press, Cambridge, U. K.

Kato, S., and A. Marshak (2009), Solar zenith and viewing geometry-dependent errors in satellite retrieved cloud optical thickness: Marine stratocumulus case, *J. Geophys. Res.*, *114*, D01202, doi:10.1029/2008JD010579.

Liang, L., L. Di Girolamo, and S. Platnick (2009), View-angle consistency in reflectance, optical thickness and spherical albedo of marine water-clouds over the northeastern Pacific through MISR-MODIS fusion, *Geophys. Res. Lett.*, *36*, L09811, doi:10.1029/2008GL037124.

Loeb, N. G., and R. Davies (1996), Observational evidence of plane parallel model biases: Apparent dependence of cloud optical depth on solar zenith angle, *J. Geophys. Res.*, *101*, 1621–1634, doi:10.1029/95JD03298.

Marshak, A., S. Platnick, T. Várnai, G. Wen, and R. F. Cahalan (2006), Impact of three-dimensional radiative effects on satellite retrievals of cloud droplet sizes, *J. Geophys. Res.*, *111*, D09207, doi:10.1029/2005JD006686.

O'Hirok, W., and C. Gautier (2005), The impact of model resolution on differences between independent column approximation and Monte Carlo estimates of shortwave surface irradiance and atmospheric heating rate, *J. Atmos. Sci.*, *62*, 2939–2951, doi:10.1175/JAS3519.1.

Ohring, G., et al. (2005), Satellite instrument calibration for measuring global climate change: Report of a workshop, *Bull. Am. Meteorol. Soc.*, *86*, 1303–1313, doi:10.1175/BAMS-86-9-1303.

Platnick, S., et al. (2003), The MODIS cloud products: Algorithms and examples from Terra, *IEEE Trans. Geosci. Remote Sens.*, *41*, 459–473, doi:10.1109/TGRS.2002.808301.

Platnick, S., et al. (2004), An initial analysis of the pixel-level uncertainties in global MODIS cloud optical thickness and effective particle size retrievals, *Proc. SPIE*, *5652*, 30–40.

Várnai, T., and A. Marshak (2003), A method for analyzing how various parts of clouds influence each other's brightness, *J. Geophys. Res.*, *108*(D22), 4706, doi:10.1029/2003JD003561.

Várnai, T., and A. Marshak (2007), View angle dependence of cloud optical thickness retrieved by Moderate Resolution Imaging Spectroradiometer (MODIS), *J. Geophys. Res.*, *112*, D06203, doi:10.1029/2005JD006912.

Zuidema, P., and K. F. Evans (1998), On the validity of the independent pixel approximation for boundary layer clouds observed during ASTEX, *J. Geophys. Res.*, *103*, 6059–6074, doi:10.1029/98JD00080.

L. Di Girolamo and L. Liang, Department of Atmospheric Sciences, University of Illinois at Urbana-Champaign, 105 South Gregory St., Urbana, IL 61801, USA. (larry@atmos.uiuc.edu)

S. Platnick, Laboratory for Atmospheres, NASA Goddard Space Flight Center, Code 613.2, Greenbelt, MD 20771, USA.